



Science Arts & Métiers (SAM)

is an open access repository that collects the work of Arts et Métiers Institute of Technology researchers and makes it freely available over the web where possible.

This is an author-deposited version published in: <https://sam.ensam.eu>
Handle ID: <http://hdl.handle.net/10985/7638>

To cite this version :

Julian SOULACROIX, Bruno MICHEL, Jean-Marie GATT, Laurent BARRALLIER, Regis KUBLER
- Micromechanical behavior of UO₂: crystalline anisotropy and associated internal stresses in polycrystals - In: Congrès français de mécanique (21 ; 2013 ; Bordeaux (Gironde), France, 2013-08-26 - Congrès français de mécanique (21 ; 2013 ; Bordeaux (Gironde) - 2013

Any correspondence concerning this service should be sent to the repository

Administrator : scienceouverte@ensam.eu



Micromechanical behavior of UO_2 : crystalline anisotropy and associated internal stresses in polycrystals

J. SOULACROIX^{a,b}, B. MICHEL^a, J.-M. GATT^a, R. KUBLER^b, L. BARRALLIER^b

a. CEA Cadarache, DEN/DEC/SESC/LSC

b. Arts et Métiers ParisTech, Aix en Provence, MSMP

Résumé :

Un modèle de plasticité cristalline a été développé et adapté à l' UO_2 . Des simulations d'essais cycliques sur agrégats polycristallins périodiques ont été réalisées avec différentes conditions aux limites. Les résultats montrent que l'anisotropie plastique de ce matériau peut expliquer en partie l'effet d'écrouissage cinématique observé expérimentalement.

Abstract :

A crystal plasticity constitutive model was developed and adjusted to UO_2 . Simulations of cyclic tests were made on periodic polycrystalline aggregates with different boundary conditions. The results show that plastic anisotropy can partly explain the kinematic hardening effect which was experimentally observed.

Mots clefs : UO_2 , kinematic hardening, crystal plasticity

1 Introduction

Uranium dioxide is the standard nuclear fuel for pressurized water reactors in France. This ceramic is manufactured by sintering. The standard shape for use in nuclear reactor is a small cylinder, also called "pellet", which measures about 8mm in diameter and 12mm in height. These pellets are then stacked into a zirconium alloy cladding, forming a rod. The fuel rods are then assembled together and these assemblies are put in the nuclear core. The mechanical behavior of the nuclear fuel during operation depends on the mechanical state of the rod (pellet and cladding), which can be related to other phenomena taking place during irradiation. A first step in the modeling approach is to study the mechanical behavior of non irradiated uranium oxide. For a temperature higher than about 1000°C and for a strain rate higher than about 1.10^{-6}s^{-1} , this material can be plastically deformed by a dislocation glide mechanism. For lower strain rate, the deformation mechanism is a diffusional process (see[6] for a complete map of the different deformations mechanisms in UO_2). In this paper, we study the effect of the plastic anisotropy on the kinematic hardening of UO_2 . Our work is based on a microscopic approach and our results suggest that the kinematic hardening effect can be explained by the intergranular interaction between neighbor grains. An evaluation of this behavior was made using a crystal plasticity constitutive model and a polycrystalline aggregate.

2 Kinematic hardening of UO_2 : experimental results

2.1 Evidence of kinematic hardening

UO_2 mechanical behavior is generally studied with a bending or a compression test. Both tests can be performed at imposed strain rate or at imposed force. In the case of bending test, the specimen is a small beam which is cut into a pellet. An evidence of kinematic hardening was observed during bending tests which were ended by a relaxing period under very small imposed force ([2, 4]). In this tests, a plastic recovery was observed, corresponding to a creep of the material in the reverse direction compared to

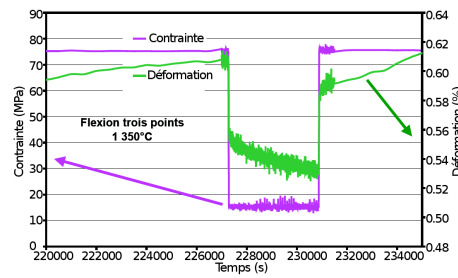


FIG. 1: Plastic recovery during bending test on a UO_2 , from [4]

the one previously observed during the first stage of testing (see fig. 1). As structural effects due to the bending configuration can not explain this phenomenon, it was assumed that there existed a back stress resulting from the initial creep test. This back stress, also called kinematic hardening, was then treated through a macroscopic constitutive relation and successfully reproduced the observed behavior ([4]).

2.2 Origin of kinematic hardening of UO_2

The measured strain rate during plastic recovery is about $5 \cdot 10^{-8} \text{s}^{-1}$ ([4]), which does not correspond to a dislocation glide mechanism ([6]). Instead, this strain rate is consistent with a diffusion mechanism, which is activated in UO_2 at high temperature and low strain rates. This mechanism may be activated by an inner stress which persists after relaxation. According to [3], this strain rate would be obtained for a compressive test with a stress of about 10 MPa. Kinematic hardening of UO_2 can not be explained by formation of dislocations cells or other dislocations structures, because they are formed for rather high strains (at least 3% according to [5]) and kinematic hardening is observed even for low strains (1%). A possible source of residual stress may be the incompatibility of deformation directions at grain boundaries. Indeed, as they are not oriented in the same direction, neighbor grains do not deform in the same direction by dislocation glide mechanism.

3 Constitutive model

3.1 A crystal plasticity model for UO_2

A crystal plasticity constitutive model was developed to evaluate the incompatibility of deformation during dislocation glide deformation. Glide systems and associated critical resolved shear stresses are known for UO_2 ([8, 1]). The two main families are $\{100\} \langle 011 \rangle$ (6 systems) and $\{110\} \langle 1\bar{1}0 \rangle$ (6 systems). The second family is harder to activate, which means that critical resolved shear stress for this family is higher than for the first one. The behavior of UO_2 is strongly dependent on stoichiometry, and our model and results are only valid for stoichiometric UO_2 . A crystal plasticity model was used and parameters were adjusted to correctly represent UO_2 (crystallography and mechanical behavior). Constitutive relations are summarized with the set of equations eq. 1, and we used parameters described in tab. 1. The value of α was chosen to cancel forest hardening effect ($\alpha = 0$), because a high forest hardening would counterbalance kinematic hardening and change the relative difference of critical resolved shear stress of the two different glide families. The elastic moduli for UO_2 at room temperature were chosen according to [9] : $C_{11} = 3.96 \cdot 10^{11} \text{Pa}$, $C_{12} = 1.21 \cdot 10^{11} \text{Pa}$, $C_{44} = 0.64 \cdot 10^{11} \text{Pa}$. No effect of temperature was considered for the elastic moduli. These constitutive relations were implemented in Cast3M (a finite element software, website : <http://www-cast3m.cea.fr>) with Mfront (a tool that allows to quickly and efficiently implement constitutive relations). For a given crystal orientation and given strain rate and temperature, the flow rate of a monocrystal can be evaluated by a finite element simulation. As expected, the UO_2 's crystallography and the difference of critical resolved shear stress between families involve an important plastic anisotropy : the maximum flow stress is about twice the minimum (fig. 2).

| notation | parameter | adjusted value / variable | unit |
|--|---|--|----------|
| $\underline{\underline{\epsilon}}_{tot}$ | total strain | variable | - |
| $\underline{\underline{\epsilon}}_{el}$ | elastic strain | variable | - |
| $\underline{\underline{\epsilon}}_{vp}$ | viscoplastic strain | variable | - |
| s | glide system index | 12 systems (2 families) | - |
| γ_s | viscoplastic strain on system s | variable | - |
| $\underline{\underline{m}}^s$ | Schmid matrices | Family 1 : $\{100\} \langle 011 \rangle$ (6 systems) | - |
| $\underline{\underline{n}}^s$ | normal vector to plane of system s | Family 2 : $\{110\} \langle 1\bar{1}0 \rangle$ (6 systems) | - |
| $\underline{\underline{b}}^s$ | normalized Burgers' vector of system s | | - |
| $\dot{\gamma}_0$ | Reference strain rate | $3.87 \cdot 10^7$ | s^{-1} |
| E_v | Activation energy for dislocation glide | 2.88 | eV |
| T | Temperature | variable | K |
| τ^s | Resolved shear stress on system s | variable | Pa |
| τ_0^s | Reference critical resolved shear stress for system s | $110 \cdot 10^6$ for $\{100\} \langle 011 \rangle$; $220 \cdot 10^6$ for $\{110\} \langle 1\bar{1}0 \rangle$ | Pa |
| τ_f^s | Forest hardening stress for system s | variable | Pa |
| k | Exponent | 5.5 | - |
| $\underline{\underline{\sigma}}$ | Stress | variable | Pa |
| α | Forest hardening coefficient | 0 for reasons explained before | - |
| μ | Shear modulus | $0.64 \cdot 10^{11}$ | Pa |
| b | Burgers' vector norm | $3.87 \cdot 10^{-10}$ | m |
| $\underline{\underline{A}}$ | Forest hardening matrix | Chosen according to [7] | - |
| ρ_s | Dislocation density | variable, initially 10^{11} | m^{-2} |
| $\underline{\underline{a}}$ | Interaction matrix | equal to $\underline{\underline{A}}$ | - |
| K | Free path coefficient | 10 | - |
| y_c | Annihilation coefficient | $15 \times b$ | m |

TAB. 1: Parameters and adjusted values for crystal plasticity model of UO₂

$$\begin{cases}
\dot{\underline{\underline{\epsilon}}}_{tot} = \dot{\underline{\underline{\epsilon}}}_{el} + \dot{\underline{\underline{\epsilon}}}_{vp} \\
\dot{\underline{\underline{\epsilon}}}_{vp} = \sum_s \dot{\gamma}^s \underline{\underline{m}}^s \\
\underline{\underline{m}}^s = \frac{1}{2} (\underline{\underline{n}}^s \otimes \underline{\underline{b}}^s + \underline{\underline{b}}^s \otimes \underline{\underline{n}}^s) \\
\dot{\gamma}^s = \dot{\gamma}_0 \exp\left(-\frac{E_v}{k_B T}\right) \left(\frac{\tau^s}{\tau_0^s + \tau_f^s}\right)^k \\
\tau^s = \underline{\underline{m}}^s : \underline{\underline{\sigma}} \\
\tau_f^s = \alpha \mu b \sqrt{\sum_r A_{rs} \rho_r} \\
\dot{\rho}^s = \frac{1}{b} \left(\frac{\sqrt{\sum_r A_{rs} \rho_r}}{K} - 2y_c \rho^s \right) |\dot{\gamma}^s|
\end{cases} \quad (1)$$

3.2 Polycrystalline aggregate

A periodic polycrystalline aggregate was generated using a Voronoi diagram based on randomly generated points. This points were chosen so as to produce grains with a given average size. Orientations were randomly chosen for each grain. The final volume consisted either of a set grains which were joined together or of a simple cubic shape (see fig 3), depending of which type of boundary conditions was used. The aggregate which was used in this study contained 90 grains and the associated meshes was made of about 80000 elements in the two cases (grains joined together or simple cubic shape).

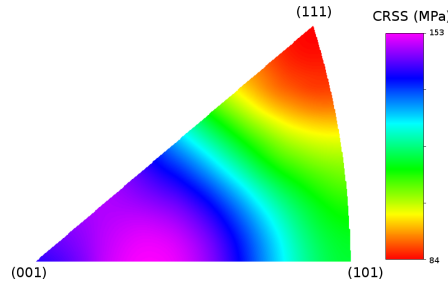


FIG. 2: Simulated flow stress represented in an inverse pole figure for UO_2 , at 1350°C , imposed strain rate of $1 \cdot 10^{-4} \text{s}^{-1}$

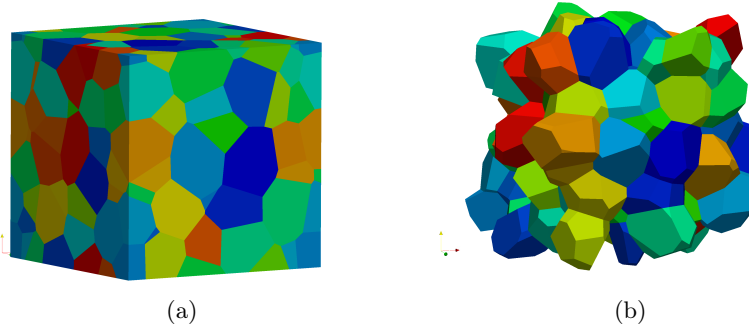


FIG. 3: Periodic polycrystalline aggregate, with a final cubic shape (a) or with whole grains joined together (b). Both geometries were generated using the same Voronoi diagram.

3.3 Boundary conditions

Two different types of boundary conditions were used. The first one is periodic boundary conditions. The second one is called “average” boundary conditions. In the case of periodic boundary conditions, the volume consists of a periodic set of grains which are joined together, so that grains are not cut by the faces of a cube. For an imposed strain, the average gradient of displacement is fully imposed : $\frac{1}{V} \int_V \nabla u dV = \nabla U = E + W$ where u is the displacement, V the aggregate’s volume, E the symmetric part of ∇U (the average deformation), and W its antisymmetric part (average rotation). This relation is fulfilled through imposed relative displacements of opposite points. For two opposite points P_1 and P_2 on the volume boundary : $u(P_2) - u(P_1) = E \cdot (X(P_2) - X(P_1))$, where $X(P_i)$ is the spatial position of point P_i . This way of imposing the average deformation ensures that the solution displacement field is periodic. Another approach of the periodic problem can be made in the case of imposed stress. In the case of “average” boundary conditions, the volume consists of a periodic polycrystalline aggregate which is cut by a cube, because the use of a simple shape makes the implementation of the method easier. For this type of conditions, the same applies than for the periodic ones : for imposed strain, the average gradient of displacement is fully imposed : $\frac{1}{V} \int_V \nabla u dV = \nabla U = E + W$ where u is the displacement, V the aggregate’s volume, E the symmetric part of ∇U (the average deformation), and W its antisymmetric part (average rotation). The difference with the periodic boundary conditions is that there is no periodic hypothesis. Indeed, for a volume whose boundaries are composed of N faces which are indexed k , Green’s theorem involves :

$$E_{ij} = \frac{1}{V} \int_V \varepsilon_{ij}(u) dV = \frac{1}{2V} \int_{\partial V} (u_i e_j + u_j e_i) \cdot n dS = \frac{1}{2V} \sum_k \int_{S_k} (u_i e_j + u_j e_i) \cdot n_k dS \quad (2)$$

n_k is the normal vector to face k . For a cubic shape oriented along the 3 axes x , y and z , the 6 surfaces can be named S_{x_0} for the surface where x is minimum, S_{x_1} for the surface where x is maximum, and the same notation for y and z . The side length is L . Then we have for example :

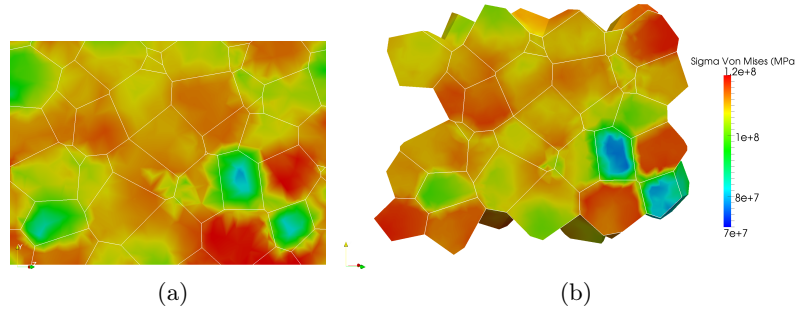


FIG. 4: Illustration of inhomogeneity of stress in an aggregate : cross-section view of the Von Mises stress in the case of the average boundary conditions (a) and periodic boundary conditions (b) for the same loading history and same periodic aggregate

$$E_{xx} = \frac{1}{L} \left(\frac{1}{L^2} \int_{S_{x_1}} u_x dS - \frac{1}{L^2} \int_{S_{x_0}} u_x dS \right) = \frac{1}{L} (\langle u_x \rangle_{S_{x_1}} - \langle u_x \rangle_{S_{x_0}}) \quad (3)$$

$$E_{xy} = \frac{1}{L} (\langle u_x \rangle_{S_{y_1}} - \langle u_x \rangle_{S_{y_0}} + \langle u_y \rangle_{S_{x_1}} - \langle u_y \rangle_{S_{x_0}}) \quad (4)$$

$\langle \cdot \rangle_S$ denotes the average value on the surface S . The same relations are true for other components of E and W . These relations can be considered as kinematic linear relations between displacement of nodes. Indeed, for a discretized geometry, we have for example :

$$\langle u_x \rangle_S = \frac{1}{L^2} \int_S u_x dS = \frac{1}{L^2} \sum_{\text{points } p \text{ on } S} \alpha^p U_x^p \quad (5)$$

where α^p is the weight of point p , and U_x^p is the displacement of point p along direction x . In a FE formulation, this weight corresponds to the total integration on the surface S of the shape functions associated to node p . All these kinematic linear relations can be directly imposed in our finite element software Cast3M. We observed numerically that this problem has a unique solution. This shows that the minimal condition to solve a mechanical problem is to know the average value of the displacement's gradient. This method could be generalized to any problem usually treated using periodic boundary conditions or other types of boundary conditions.

4 Simulation results

Several cyclic tests were simulated. The first stage of the test is a compression test. Then, after 1% of total ZZ strain, the loading is reversed and a tensile test is simulated, until the total ZZ strain reaches zero. All these tests were simulated with an imposed strain rate of $10^{-4} s^{-1}$ and a temperature of $1350^\circ C$. We made the same simulations (same mesh, same loading) using either linear elements or quadratic elements, so that the effect of elements' type was determined in our case. There seems to be no significant difference between the results obtained either with average boundary conditions or periodic boundary conditions, as illustrated by fig. 5. During the elastic deformation stage, the two responses even seem to be actually equal. A more precise study will have to be made to compare these two methods and conclude on the differences between the two methods. The value of the stress at the very beginning of plastic deformation (i.e. the yield stress) was defined as the value of the stress for a plastic deformation equal to $2 \cdot 10^{-5} = 0.002\%$. In the case of a cyclic loading, we measured this value at the first loading stage, and then we measured it another time during the reverse loading stage. Hence, the difference between these two values is the value of the observed kinematic hardening (see fig. 5). Our numerical evaluation of kinematic hardening gave a value between 8 MPa (for quadratic elements) and 12.5 MPa (for linear elements) (fig. 5). This means that even at zero imposed stress, UO_2 deforms just as it was under a tensile stress of about 10 MPa. This value is consistent with the value given in paragraph 2.2.

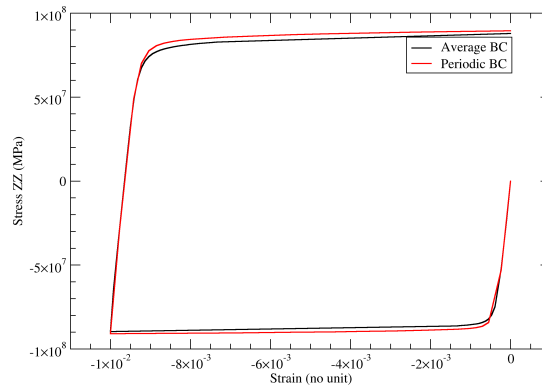


FIG. 5: Simulation of a cyclic test : the ZZ component of the stress as a function of ZZ imposed total strain for average and periodic boundary conditions, in the case of linear elements, for our aggregate (strain rate = $10^{-4} s^{-1}$, $T = 1350^{\circ}C$).

5 Conclusions

The behavior of crystalline UO_2 was modeled through a crystal plasticity constitutive model and the mechanical behavior of an aggregate was simulated with a finite elements method. Different boundary conditions and different types of elements were used. Our simulations have shown that the plastic anisotropy of crystalline UO_2 generates incompatibilities between neighbor grains during a macroscopic compressive test. These incompatibilities result into a localization of stress, which can be macroscopically reduced to a kinematic hardening. The value of the calculated kinematic hardening is consistent with the experimental results. The diffusion process which occurs during plastic recovery (see fig. 1) has not been modeled, because it needs a specific diffusion constitutive model. The effect of the aggregate geometry still needs to be studied to ensure that our geometry was representative of any UO_2 microstructure. The influence of material parameters (relative difference of critical stresses between the two glide families) and of strain rate need to be also studied.

Références

- [1] W.M. Armstrong, A.R. Causez, and W.R. Sturrock. Creep of single-crystal UO_2 . *Journal of Nuclear Materials*, 19 :42–49, 1966.
- [2] W.M. Armstrong, W.R. Irvine, and R.H. Martinson. Creep deformation of stoichiometric uranium dioxide. *Journal of Nuclear Materials*, 7 :133–141, 1962.
- [3] B. Burton and G.L. Reynolds. The influence of deviation from stoichiometric composition on the diffusional creep of uranium dioxide. *Acta Metallurgica*, 21 :1641–1647, 1973.
- [4] C. Colin. *Etude du fluage du dioxyde d'uranium : caractérisation par essais de flexion et modélisation mécanique*. PhD thesis, Ecole Nationale Supérieure des Mines de Paris, 2003.
- [5] F. Dherbey. *Déformation a chaud du dioxyde d'uranium polycristallin*. PhD thesis, Institut National Polytechnique de Grenoble, 2000.
- [6] H.J. Frost and M.F. Ashby. *Deformation-mechanism maps : the plasticity and creep of metals and ceramics*. Pergamon Press, 1982.
- [7] L. Kubin, B. Devincre, and T. Hoc. Modeling dislocation storage rates and mean free paths in face-centered cubic crystals. *Acta Materialia*, 56 :6040–6049, 2008.
- [8] E.J. Rapperport and A.M. Huntress. Deformation modes of single crystal uranium dioxide from $700^{\circ}C$ to $1900^{\circ}C$. *NMI-1242 Metallurgy and ceramics*, 1960.
- [9] J.B. Watchman and J.L. Bates. Elastic constants of single crystal UO_2 at $25^{\circ}C$. *Journal of nuclear materials*, 16 :39–41, 1965.